

UCSF

UC San Francisco Previously Published Works

Title

Blue fluorescent amino acid for biological spectroscopy and microscopy

Permalink

<https://escholarship.org/uc/item/6px2d982>

Journal

Proceedings of the National Academy of Sciences of the United States of America, 114(23)

ISSN

0027-8424

Authors

Hilaire, Mary Rose
Ahmed, Ismail A
Lin, Chun-Wei
et al.

Publication Date

2017-06-06

DOI

10.1073/pnas.1705586114

Peer reviewed



Blue fluorescent amino acid for biological spectroscopy and microscopy

Mary Rose Hilaire^{a,1}, Ismail A. Ahmed^{b,1}, Chun-Wei Lin^a, Hyunil Jo^c, William F. DeGrado^{c,2}, and Feng Gai^{a,d,2}

^aDepartment of Chemistry, University of Pennsylvania, Philadelphia, PA 19104; ^bDepartment of Biochemistry and Molecular Biophysics, University of Pennsylvania, Philadelphia, PA 19104; ^cDepartment of Pharmaceutical Chemistry, University of California, San Francisco, CA 94158; and ^dUltrafast Optical Processes Laboratory, University of Pennsylvania, Philadelphia, PA 19104

Contributed by William F. DeGrado, April 20, 2017 (sent for review February 20, 2017; reviewed by Jacob W. Petrich and Dongping Zhong)

Many fluorescent proteins are currently available for biological spectroscopy and imaging measurements, allowing a wide range of biochemical and biophysical processes and interactions to be studied at various length scales. However, in applications where a small fluorescence reporter is required or desirable, the choice of fluorophores is rather limited. As such, continued effort has been devoted to the development of amino acid-based fluorophores that do not require a specific environment and additional time to mature and have a large fluorescence quantum yield, long fluorescence lifetime, good photostability, and an emission spectrum in the visible region. Herein, we show that a tryptophan analog, 4-cyanotryptophan, which differs from tryptophan by only two atoms, is the smallest fluorescent amino acid that meets these requirements and has great potential to enable *in vitro* and *in vivo* spectroscopic and microscopic measurements of proteins.

fluorescence protein | fluorescence probe | unnatural amino acid | imaging

Of the amino acids that are inherently responsible for the fluorescence of proteins, tyrosine (Tyr), tryptophan (Trp), and phenylalanine (Phe), Trp is the most widely used fluorescence reporter of protein structure, function, and dynamics, as its fluorescence quantum yield (QY) is comparatively large and is also sensitive to environment (1–3). However, Trp absorbs/emits in the UV wavelength region and has low photostability. Combined, these factors render this naturally occurring fluorescent amino acid hardly useful as a fluorophore for single-molecule measurements (4) and imaging applications, especially under *in vivo* conditions. For this reason, significant efforts have been devoted to identifying small unnatural fluorophores (5–11) that could overcome this limitation. So far, only naphthalene-based fluorophores, such as prodan (8, 9) and aladan (11) have been shown to be useful in this regard. However, these fluorophores are not structurally based on any naturally occurring amino acids and are larger in size than Trp, making them less attractive in applications where there are stringent requirements for the fluorophore size and structure. Therefore, the development of a smaller, ideally amino acid-based, fluorophore that does not require additional time to mature, have a large fluorescence QY, long fluorescence lifetime, good photostability, and an emission spectrum in the visible range, would enhance biological research. Herein, we show that a Trp analog, 4-cyanotryptophan (4CN-Trp), meets these requirements and has great potential to expand biological fluorescence spectroscopy and microscopy into additional territory.

Many past studies have focused on Trp-based unnatural amino acids, including azatryptophans (5, 6, 12) and various indole-ring substituted analogs (13–16), aiming to identify useful biological fluorophores. Whereas some Trp analogs indeed exhibit improved fluorescent properties over Trp, none of them has found broad applications due to certain photophysical limitations. Recently, Talukder et al (15) showed that 6-cyanotryptophan (6CN-Trp) and 7-cyanotryptophan (7CN-Trp) have a significantly increased QY (about 0.5 in methanol) compared with that of Trp (about 0.15 in water), suggesting that cyanotryptophans

are potential candidates that meet the aforementioned requirements. However, the emission maxima of 6CN-Trp and 7CN-Trp in methanol are centered at 370 and 390 nm, respectively, making them less attractive as visible fluorophores. As shown (Fig. 1), the absorption and emission spectra of 4-cyano-indole (4CNI), the sidechain of 4CN-Trp, are significantly shifted from those of indole (or Trp) and, in particular, an emission maximum of 405 nm suggests that 4CN-Trp could be a viable candidate for the aforementioned amino acid-based fluorophores. Indeed, our results confirm that 4CN-Trp emits in the blue region of the visible spectrum with a large QY (>0.8) and has a long fluorescence lifetime (13.7 ns), a reasonably large molar extinction coefficient ($\sim 6,000 \text{ M}^{-1}\cdot\text{cm}^{-1}$), and good photostability. Taken together, these qualities make 4CN-Trp an attractive blue fluorescent amino acid (BFAA) for biological spectroscopy and microscopy.

Results and Discussion

Fluorescence Quantum Yield Measurements. To explore the feasibility of using 4CN-Trp as a biological fluorescence emitter, we first examined the QY of its fluorophore, 4-cyano-indole (4CNI). As shown (Fig. 1B), the absorption spectrum of 4CNI in water is broader than and red shifted from that of Trp, making it possible to prepare its electronically excited and fluorescent state using an excitation wavelength (λ_{ex}) of greater than 310 nm, without exciting any of the naturally occurring fluorescent amino acids. This constitutes one of the key advantages of using 4CNI-based amino acid fluorophores. Similarly, the fluorescence spectrum of 4CNI in water is red shifted from that of indole (Fig. 1C), with a maximum emission wavelength of 405 nm. In addition, and perhaps more importantly, the integrated fluorescence intensity of 4CNI is much larger than that of indole, indicating that 4CNI has a much larger fluorescence QY than indole. To determine the QY of 4CNI, we quantitatively compared its fluorescence

Significance

Herein, we report a tryptophan-based fluorophore that emits in the visible spectral region when excited with 355-nm light. Because this blue fluorescent amino acid has a small size and affords unique photophysical properties, we expect that it will find use in various biological studies, especially in spectroscopic and/or microscopic measurements where an amino acid-sized fluorescence reporter is required.

Author contributions: M.R.H. and F.G. designed research; M.R.H., I.A.A., C.-W.L., and H.J. performed research; and M.R.H., W.F.D., and F.G. wrote the paper.

Reviewers: J.W.P., Iowa State University; and D.Z., The Ohio State University.

The authors declare no conflict of interest.

¹M.R.H. and I.A.A. contributed equally to this work.

²To whom correspondence may be addressed. Email: william.degrado@ucsf.edu or gai@sas.upenn.edu.

This article contains supporting information online at www.pnas.org/lookup/suppl/doi:10.1073/pnas.1705586114/-DCSupplemental.

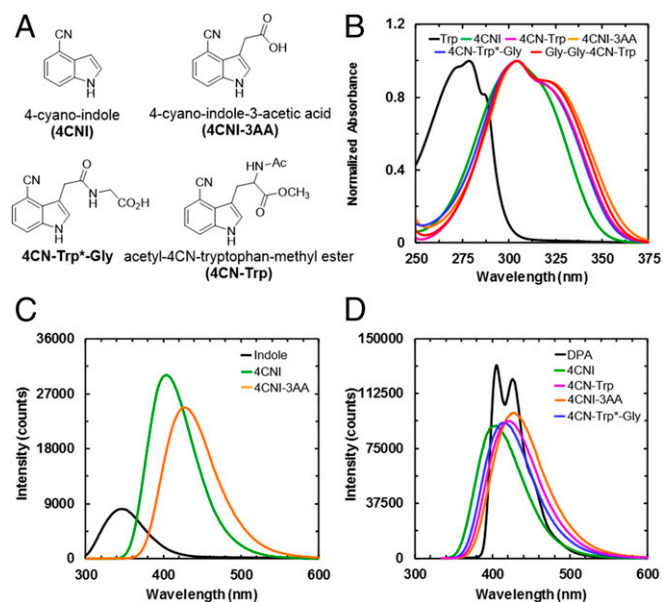


Fig. 1. (A) Structures of 4CNI, 4CNI-3AA, 4CN-Trp, and 4CN-Trp*-Gly, as indicated. (B) Absorption spectra of Trp, 4CNI, 4CNI-3AA, 4CN-Trp, 4CN-Trp*-Gly, and Gly-Gly-4CN-Trp, as indicated. (C) Comparison of the fluorescence spectrum of indole with those of 4CNI and 4CNI-3AA. These spectra were obtained with an excitation wavelength of 270 nm at 25 °C and the optical densities of all of the samples at 270 nm were equal. (D) Comparison of the fluorescence spectrum of DPA with those of 4CNI, 4CNI-3AA, 4CN-Trp, and 4CN-Trp*-Gly. These spectra were obtained with an excitation wavelength of 325 nm at 25 °C, and the optical densities of all of the samples at 325 nm were equal.

spectrum with that of Trp or 9,10-diphenylanthracene (DPA) (Fig. 1D) using the following relationship (17):

$$QY_S = QY_R \frac{I_S A_R n_S^2}{I_R A_S n_R^2}, \quad [1]$$

where I is the integrated fluorescence intensity, A is the optical density of the fluorophore at λ_{ex} , n is the index of refraction of the solvent, and the subscripts S and R represent the sample and reference, respectively. Both Trp and DPA are commonly used fluorescence QY standards (18), with a QY of 0.15 for Trp in water at $\lambda_{\text{ex}} = 270$ nm and 0.9 (0.97) for DPA in cyclohexane at $\lambda_{\text{ex}} = 325$ nm (355 nm). Therefore, for an λ_{ex} of 270 nm, we used Trp as the reference, whereas for an λ_{ex} of equal to or larger than 325 nm, we used DPA as the reference.

As indicated (Table 1), at λ_{ex} of 270 nm, the QY of 4CNI was determined to be 0.85 ± 0.13 . To the best of our knowledge, this value is the largest among the reported QY values of all indole (the sidechain of Trp) derivatives, signifying the potential utility of 4CNI as a biological fluorophore. Moreover, the high QY of 4CNI is preserved at even longer excitation wavelengths, determined using DPA as a reference (Table 1). Taken together, these results suggest that 4CN-Trp could be a bright enough fluorophore for biological single-molecule and imaging experiments, excited in a spectral region separated from that of other intrinsic fluorescent amino acids.

Because the photophysical properties of 4CNI could change when incorporated in an amino acid or peptide environment, we further quantified the absorption and emission spectra of 4CN-Trp, Gly-Gly-4CN-Trp, 4-cyano-indole-3-acetic acid (4CNI-3AA), and 4CN-Trp*-Gly. (For nomenclature see Fig. 1A; 4CN-Trp and Gly-Gly-4CN-Trp were evaluated as the corresponding *N*-acetyl methyl esters, whereas the other peptides are assessed as the free carboxylates.) 4CN-Trp was synthesized as described in *Materials*

and *Methods*, whereas the corresponding 4CN-Trp* peptide derivatives were prepared from the commercially available and relatively inexpensive 4CNI-3AA, which can be conveniently appended to the N-terminal end of a peptide (Fig. 1A). As shown (Fig. 1), the absorption and emission spectra of 4CN-Trp, 4CNI-3AA, Gly-Gly-4CN-Trp, and 4CN-Trp*-Gly in water are very similar to each other, suggesting that 4CNI-3AA can be used as an alternative of 4CN-Trp. Furthermore, their absorption spectra extend further to the longer wavelengths in comparison with that of 4CNI, with a second maximum at 325 nm. These absorption characteristics are important, as they render the use of various commercially available lasers, such as the 355-nm YAG laser or the 325-nm HeCd laser commonly used in flow cytometry, to excite the 4CN-Trp fluorophore.

As indicated (Fig. 1C), the fluorescence spectra of 4CN-Trp, 4CNI-3AA, Gly-Gly-4CN-Trp, and 4CN-Trp*-Gly have a peak wavelength of greater than 415 nm, making the 4CN-Trp chromophore a true blue fluorescence emitter. Perhaps more importantly, their fluorescence QYs in water at 25 °C are larger than 0.80 when an λ_{ex} of 325 nm was used (Table 1), confirming that 4CN-Trp is a highly emissive BFAA. Further measurements on 4CN-Trp*-Gly in a 20 mM phosphate buffer (pH 7.2) at 37 °C and in tetrahydrofuran (THF), an aprotic solvent commonly used to mimic the hydrophobic interior of proteins because of its low dielectric constant, show that the QY is only decreased to about 0.6 (Table 1) under these conditions. This is a key finding as it indicates that the strong fluorescence emission property 4CN-Trp is maintained under physiological conditions and also in a dehydrated environment. It is well known that several amino acids (19), including methionine (Met) (20), can quench Trp fluorescence. However, as shown (Table 1 and Fig. S1A), the QY of 4CN-Trp*-Met is similar to that of 4CN-Trp*-Gly. This result suggests that the fluorescence QY of 4CN-Trp may not be as sensitive to nearby residues as Trp is. Taken together, the above results suggest that the brightness of a 4CNI fluorophore in a protein will not be significantly affected by its location and can be attached to either a solvent-exposed or buried position.

Fluorescence Lifetime Measurements. In applications where the fluorophore of interest is imbedded in a heterogeneous and light-scattering medium, such as cells, time-based fluorescence measurements can be advantageous. Therefore, we further determined the fluorescence decay kinetics of 4CNI, 4CNI-3AA, 4CN-Trp, Gly-Gly-4CN-Trp, and 4CN-Trp*-Gly. As shown (Fig. S2), 4CNI, 4CNI-3AA, and 4CN-Trp*-Gly in water afford single-exponential fluorescence decay kinetics with, more interestingly, a long lifetime (e.g., 12.6 ns for 4CN-Trp*-Gly) (Table 1). The fluorescence decay kinetics of 4CN-Trp and Gly-Gly-4CN-Trp show a predominant long lifetime component (~ 13.6 ns; $\sim 95\%$), and a small 5% shorter lifetime component (~ 1.8 ns) (Table 1). It is possible that this double-exponential decay behavior arises from different 4CN-Trp rotamers, as proposed for interpreting the nonsingle-exponential fluorescence decay kinetics of Trp (17). However, the fact that both the C and N termini of 4CN-Trp and Gly-Gly-4CN-Trp used in the current study are capped and that the fluorescence of 4CN-Trp*-Gly, which has an amide bond, decays in a single-exponential manner, argue against this possibility. Therefore, we tentatively attribute the shorter lifetime component to an impurity that cannot be removed by the purification methods used. One likely candidate for this impurity is Trp, a byproduct of the synthesis of 4CN-Trp. Regardless of the origin of this minor component, the prolonged fluorescence lifetimes of these model systems are consistent with their high QY values. In addition, they demonstrate that 4CN-Trp could be a useful fluorophore in time-gated fluorescence imaging applications as its long fluorescence lifetime allows more efficient elimination of the autofluorescence background (~ 6 ns) in experiments involving cells (21). As shown (Table 1 and Fig. S2), the long fluorescence lifetime of 4CN-Trp*-Gly (7.6 ns) is also

Table 1. Fluorescence lifetime (τ) and QYs measured for 4CNI, 4CN-Trp, and their derivatives under different excitation wavelengths, temperatures (T), and solution conditions

Sample	Solvent	T ($^{\circ}\text{C}$)	τ (ns) (%Amp)	QY 270 nm	QY 325 nm	QY 355 nm
4CNI	H ₂ O	25	9.1 (100)	0.85 ± 0.13	0.78 ± 0.03	0.64 ± 0.07
4CNI-3AA	H ₂ O	25	13.5 (100)	0.71 ± 0.04	$0.83 \pm 0.05^{\dagger}$	0.91 ± 0.14
4CN-Trp*-Gly	H ₂ O	25	12.6 (100)	0.73 ± 0.10	0.84 ± 0.09	0.82 ± 0.05
4CN-Trp*-Gly	THF	25	7.6 (100)	—	0.62 ± 0.01	0.56 ± 0.06
4CN-Trp*-Gly	Buffer [‡]	37	—	—	0.64 ± 0.05	0.74 ± 0.03
4CN-Trp*-Met	H ₂ O	25	12.2 (100)	—	0.75^{\S}	—
4CN-Trp	H ₂ O	25	13.7 (95)	—	$0.88 \pm 0.06^{\dagger}$	—
			1.9 (5)	—	—	—
Gly-Gly-4CN-Trp	H ₂ O	25	13.6 (93)	—	$0.89 \pm 0.05^{\dagger}$	—
			1.7 (7)	—	—	—

[†]Measurements made using the gradient method as described in *SI Materials and Methods*.

[‡]20 mM phosphate buffer, pH 7.2.

[§]QY determined relative to 4CN-Trp*-Gly.

maintained in THF, indicating that its fluorescence utility is not significantly compromised even when sequestered in a hydrophobic environment in proteins, making it a versatile fluorescence probe. In addition, the fluorescence lifetime of 4CN-Trp*-Met (12.2 ns) is nearly identical to that of 4CN-Trp*-Gly (Table 1 and Fig. S1B), corroborating the conclusion reached above that Met does not quench the fluorescence of the 4CNI fluorophore.

Photostability Measurement. A key factor determining the utility of a fluorophore in single-molecule spectroscopy or confocal imaging application is its photostability. Therefore, we attempted to determine the photostability of the fluorophore in 4CN-Trp*-Gly. However, there are no standard practices to measure the photobleaching rate, as this rate depends upon many factors, including the source intensity (arc lamp or laser), the excitation filters, and the type of experiment being performed (e.g., single-molecule versus bulk) (22), which complicates comparisons between fluorophores measured at different times and places. Therefore, we compared the photobleaching kinetics of 4CN-Trp*-Gly and the enhanced blue fluorescent protein (EBFP) (23) under identical conditions (i.e., both samples have the same integrated absorbance at the excitation wavelength). As indicated (Fig. 2A), after exposing the sample to 355-nm light, derived from a Jobin Yvon Horiba Fluorolog 3.10 fluorometer equipped with a 450 W xenon arc lamp with the excitation slit width set at 5 nm, the fluorescence intensity of 4CN-Trp*-Gly in water at 25 $^{\circ}\text{C}$ decreased only $\sim 25\%$ from its initial value in 10 h, whereas that of EBFP decreased $\sim 75\%$ over the same time period. Thus, these results demonstrate that the 4CN-Trp fluorophore is more resistant to photobleaching than EBFP, a property very useful in measurements, such as time-lapse imaging, wherein the same set of fluorophores is required to be exposed to excitation light for a relatively long period.

Furthermore, to provide a direct visual comparison between the fluorescence intensities of these two fluorophores, we took pictures of a 50-nM 4CN-Trp*-Gly sample and a 50-nM EBFP sample. As shown (Fig. 2B), both samples emit blue light of comparable brightness when excited with the same light ($\lambda_{\text{ex}} = 340$ nm, derived from the aforementioned fluorometer), substantiating the notion that 4CN-Trp could be used as an alternative to fluorescent proteins.

Fluorescence Imaging Application. In a proof-of-principle imaging experiment, we used the 4CNI fluorophore to monitor the distribution of a cytotoxic and antimicrobial peptide (AMP) inside HEK293T/17 cells. Specifically, we appended a 4CNI fluorophore to the N terminus of an AMP, Mastoparan X (MpX) (24), via reacting 4CNI-3AA with MpX using the same synthesis method used to make 4CN-Trp*-Gly (the resultant peptide is

hereafter referred to as 4CN-Trp*-MpX). First, we used a commercial wide-field microscope (Olympus IX71) equipped with a 60 \times water objective and a 100-W Hg lamp to test whether the fluorescence is strong enough under conditions commonly used in similar imaging applications (i.e., 1–10 μM peptide and $\sim 3,000$ cells). In comparison with the control (Fig. 3A and D), it is apparent that the fluorescence image (Fig. 3F) acquired with 10 μM peptide allows a clear visualization of the distribution of 4CN-Trp*-MpX inside the HEK cells, which shows that this AMP distributes throughout the cell except in the nucleus. This result indicates, as also observed for other peptides (25, 26), that MpX is not only able to bind to cell membranes but can also permeate into the cytosol. Whereas, as expected, the fluorescence image obtained with 1 μM peptide (Fig. 3E) is much fainter, it still provides enough contrast to allow a rough visual inspection of the AMP distribution, in comparison with the control (Fig. 3A and D). This is a remarkable result, considering the fact that the commercial optical filter sets available on the microscope limited the shortest excitation wavelength to 355 nm, which locates at the tail region of the absorption spectrum of the amino acid fluorophore (Fig. 1B). In other words, an excitation wavelength of 330 nm, where 4CN-Trp exhibits a maximum absorbance, would substantially increase the image contrast or render the use of lower peptide concentrations. Furthermore, time-lapse microscopic measurements showed that useful images can still be obtained even after exposing the AMP-bound cells to the excitation light for over 15 min (Fig. S3), consistent with the notion that 4CN-Trp is a highly photostable fluorophore.

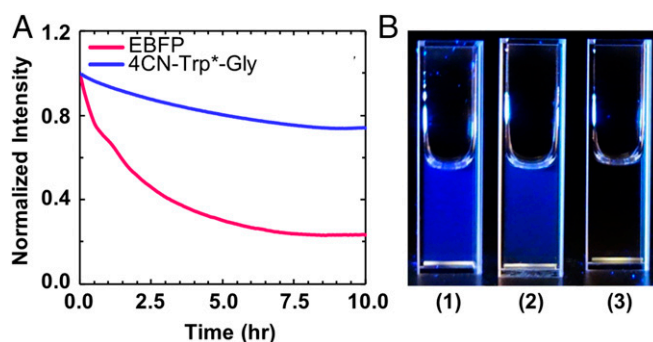


Fig. 2. (A) Photobleaching kinetics of an EBFP sample (pink) and a 4CN-Trp*-Gly sample (blue). For both cases, the photobleaching light at 355 nm was derived from a Fluorolog 3.10 fluorometer with the excitation slit width set at 5 nm. (B) Pictures of a 50-nM 4CN-Trp*-Gly sample (1), a 50-nM EBFP sample (2), and water (3) under illumination of 340-nm light, taken using a Sony RX10 camera.

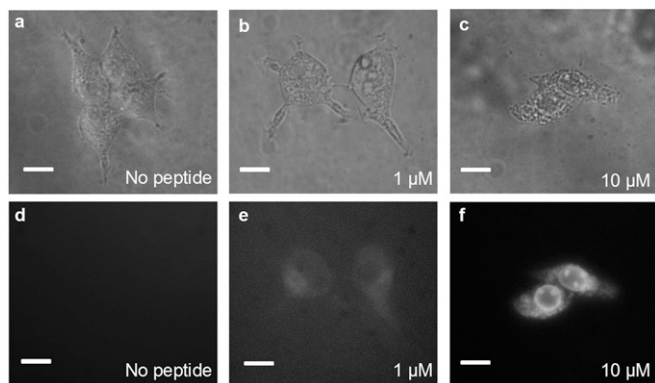


Fig. 3. Bright-field (A–C) and fluorescence (D–F) images of HEK293T/17 cells obtained on an Olympus IX71 microscope, in the presence and absence of 4CN-Trp*-MpX at the indicated concentrations. (All scale bars, 10 μ m.)

It is known that AMPs can cause cell death via two mechanisms, necrosis and apoptosis (27). Necrosis results in cell membrane rupture and loss of cellular content, whereas apoptosis leads to cell fragmentation and formation of smaller apoptotic bodies that still contain functional organelles. It is apparent that interaction with MpX leads to HEK cell death, as the morphology of the cell becomes more circular and shrinks in size upon increasing 4CN-Trp*-MpX concentration (Fig. 3). To determine the mechanism of action of MpX toward HEK cells and to also verify the potential utility of 4CN-Trp in confocal microscopy, next we used a home-built confocal microscope to image the “products” arising from AMP-induced HEK cell death. For comparison, we used the same cell sample used to generate the wide-field image in Fig. 3E (i.e., in the presence of 1 μ M 4CN-Trp*-MpX) but waited \sim 10 more hours before confocal measurements to ensure cell death throughout the entire population. As shown (Fig. 4A), large-area confocal images acquired with low spatial resolution suggest that the HEK cells in this case die via the apoptosis pathway, as manifested by formation of membrane blebs and small vesicle-like particles (27). Further evidence supporting this notion comes from a confocal image acquired with a higher spatial resolution (Fig. 4B), which clearly shows the existence of micrometer-sized components that can interact with 4CN-Trp*-MpX within a circular bleb. It is noteworthy that our confocal microscope used a 340-nm LED as the excitation source, which is less focusable and has a low power (>6 μ W) compared with a coherent laser beam. Additionally, the photon counting detector in the current confocal setup is optimized to detect photons in the red region of the visible spectrum, with less than 20% efficiency in the fluorescence spectral region of 4CN-Trp*-MpX. Therefore, we believe that better 4CN-Trp fluorescence confocal images (i.e., better resolution and contrast) can be obtained when a coherent light excitation source and a detector optimized to detect blue fluorescence are used.

Conclusions

Because of its relatively large molar absorptivity and fluorescence QY, Trp has become the natural target or template of many previous efforts to develop amino acid-based fluorophores for biological applications. Whereas several Trp-based fluorescent unnatural amino acids have been shown to offer improved spectroscopic utility over Trp (5–7), none of them has been proven to be useful for in vivo imaging applications. Herein, we have shown that by replacing the hydrogen atom at the fourth position of the indole ring of Trp with a nitrile group, the resultant unnatural amino acid, 4CN-Trp, exhibits unique photophysical properties: it has an absorption spectrum peaked at \sim 325 nm, an emission spectrum peaked at \sim 420 nm, a large fluorescence QY (0.8–0.9), a long fluorescence lifetime (13.7 ns),

and good photostability. Combined, these properties make 4CN-Trp an exceedingly useful fluorescent reporter for in vitro and in vivo spectroscopic and microscopic applications. Whereas 4CN-Trp has not yet been biosynthetically incorporated into protein systems, we do not believe this is a difficult technological undertaking as various methods (13, 15, 28, 29) have been developed to site-specifically incorporate other Trp analogs, such as 6CN-Trp and 7CN-Trp (15), hydroxytryptophans (13), azatryptophans (13), and methyltryptophans (29), into the proteins of interest. Furthermore, we believe that the current study is only the first step in exploring the potential utility of 4CN-Trp in biological research; we expect that future studies will investigate its applicability in single-molecule spectroscopy and multiphoton microscopy. In comparison with Trp, which poses several challenges in these types of applications (30–32), 4CN-Trp has the advantages of being more photostable and having an excitation spectrum that is readily accessible by a typical femtosecond Ti:Sapphire laser (700–1,000 nm). Moreover, besides its attractive photophysical properties, the small size of 4CN-Trp, which only differs from its naturally occurring counterpart by two atoms, will make this BFAA especially useful in applications where a minimally perturbing fluorescence probe is required. Finally, it is worth mentioning that further experimental and theoretical studies are needed to understand why 4CN-Trp possesses rather unique photophysics, in comparison with other tryptophan derivatives.

Materials and Methods

Small molecules were purchased from either Acros Organics (Trp, 4CNI, and DPA), Ark Pharm (4CNI-3AA), or Sigma (indole) and used as received. To the best of our knowledge, 4-cyano-L-tryptophan was currently not available commercially. Therefore, we synthesized 4-cyano-L-tryptophan by first synthesizing *N*-alpha-Boc-4-bromo-L-tryptophan methyl ester, which was prepared from the readily available 4-bromo-L-tryptophan by methylation using TMSCl_2N_2 followed by Boc protection using the reagents Boc_2O and triethylamine. Palladium-catalyzed cyanation of the *N*-alpha-Boc-4-bromo-L-tryptophan methyl ester was performed under mild condition (40 $^\circ\text{C}$, overnight) with the ligand developed by Cohen and Buchwald (33). Subsequent Boc deprotection by TFA [50% in dichloromethane (DCM)] provided the amine, which was acetylated using acetic anhydride in dimethylformamide (DMF). High performance liquid chromatography (HPLC) furnished the purified 4CN-tryptophan derivative as the acetyl, methyl ester (designated 4CN-Trp). For the solution phase peptide synthesis, the amine of 4-cyano-L-tryptophan methyl ester was coupled to Fmoc-Gly-Gly-OH using *O*-(6-Chlorobenzotriazol-1-yl)-*N,N,N,N'*-tetramethyluronium hexafluorophosphate (HCTU) and *N,N*-diisopropylethylamine (DIPEA). The Fmoc group was removed by diethylamine and the amide was acetylated using acetic anhydride in DMF to furnish the *N*-acetyl methyl ester of the tripeptide Gly-Gly-4CN-Trp after HPLC purification. Steady-state fluorescence spectra were collected on a Jobin Yvon Horiba Fluorolog 3.10 fluorometer. Fluorescence decay kinetics were

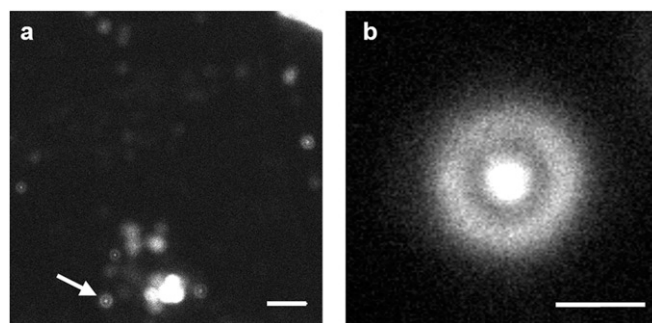


Fig. 4. Representative confocal microscopic images of HEK293T/17 cells that have been incubated with 1 μ M 4CN-Trp*-MpX for \sim 10 h, obtained with a scanning step size of 100 nm (A) and 50 nm (B). (Scale bar in A, 10 μ m; in B, 2 μ m.) Many blebs and other cellular debris can be seen in A, indicating that the HEK cells have died. The higher-resolution image in B corresponds to the bleb indicated by the white arrow in A.

collected on a home-built time correlated single photon counting (TCSPC) setup, using an excitation of 270 nm. Wide-field fluorescence images were acquired on an Olympus IX71 microscope equipped with a 100-W Hg lamp and a 60 \times water objective. Confocal images were acquired on a home-built stage-scanning confocal microscope. Additional details of 4CN-Trp and Gly-Gly-4CN-Trp synthesis, sample preparation (Fig. S4), fluorescence measurements (Fig. S5), and imaging experiments are given in *SI Materials and Methods*.

1. Royer CA (2006) Probing protein folding and conformational transitions with fluorescence. *Chem Rev* 106:1769–1784.
2. Zhong D (2009) Hydration dynamics and coupled water-protein fluctuations probed by intrinsic tryptophan. *Advances in Chemical Physics*, ed Rice SA (Wiley, Hoboken, NJ), pp 83–149.
3. Callis PR (2014) Binding phenomena and fluorescence quenching. II: Photophysics of aromatic residues and dependence of fluorescence spectra on protein conformation. *J Mol Struct* 1077:22–29.
4. Roy R, Hohng S, Ha T (2008) A practical guide to single-molecule FRET. *Nat Methods* 5:507–516.
5. Smirnov AV, et al. (1997) Photophysics and biological applications of 7-azaindole and its analogs. *J Phys Chem B* 101:2758–2769.
6. Lepthien S, Hoels MG, Merkel L, Budisa N (2008) Azatryptophans endow proteins with intrinsic blue fluorescence. *Proc Natl Acad Sci USA* 105:16095–16100.
7. Moroz YS, Binder W, Nygren P, Caputo GA, Korendovych IV (2013) Painting proteins blue: β -(1-azulenyl)-L-alanine as a probe for studying protein-protein interactions. *Chem Commun (Camb)* 49:490–492.
8. Summerer D, et al. (2006) A genetically encoded fluorescent amino acid. *Proc Natl Acad Sci USA* 103:9785–9789.
9. Chatterjee A, Guo J, Lee HS, Schultz PG (2013) A genetically encoded fluorescent probe in mammalian cells. *J Am Chem Soc* 135:12540–12543.
10. Hamada H, et al. (2005) Position-specific incorporation of a highly photodurable and blue-laser excitable fluorescent amino acid into proteins for fluorescence sensing. *Bioorg Med Chem* 13:3379–3384.
11. Cohen BE, et al. (2002) Probing protein electrostatics with a synthetic fluorescent amino acid. *Science* 296:1700–1703.
12. Talukder P, et al. (2014) Tryptophan-based fluorophores for studying protein conformational changes. *Bioorg Med Chem* 22:5924–5934.
13. Ross JBA, Szabo AG, Hogue CWV (1997) Enhancement of protein spectra with tryptophan analogs: Fluorescence spectroscopy of protein-protein and protein-nucleic acid interactions. *Methods Enzymol* 278:151–190.
14. Lotte K, Plessow R, Brockhinke A (2004) Static and time-resolved fluorescence investigations of tryptophan analogues: A solvent study. *Photochem Photobiol Sci* 3: 348–359.
15. Talukder P, et al. (2015) Cyanotryptophans as novel fluorescent probes for studying protein conformational changes and DNA-protein interaction. *Biochemistry* 54: 7457–7469.
16. Markiewicz BN, Mukherjee D, Troxler T, Gai F (2016) Utility of 5-cyanotryptophan fluorescence as a sensitive probe of protein hydration. *J Phys Chem B* 120:936–944.
17. Lakowicz JR (1999) *Principles of Fluorescence Spectroscopy* (Springer, New York), 2nd Ed.
18. Suzuki K, et al. (2009) Reevaluation of absolute luminescence quantum yields of standard solutions using a spectrometer with an integrating sphere and a back-thinned CCD detector. *Phys Chem Chem Phys* 11:9850–9860.
19. Chen Y, Barkley MD (1998) Toward understanding tryptophan fluorescence in proteins. *Biochemistry* 37:9976–9982.
20. Yuan T, Weljie AM, Vogel HJ (1998) Tryptophan fluorescence quenching by methionine and selenomethionine residues of calmodulin: Orientation of peptide and protein binding. *Biochemistry* 37:3187–3195.
21. Berezin MY, Achilefu S (2010) Fluorescence lifetime measurements and biological imaging. *Chem Rev* 110:2641–2684.
22. Shaner NC, Steinbach PA, Tsien RY (2005) A guide to choosing fluorescent proteins. *Nat Methods* 2:905–909.
23. Yang T-T, et al. (1998) Improved fluorescence and dual color detection with enhanced blue and green variants of the green fluorescent protein. *J Biol Chem* 273:8212–8216.
24. Wakamatsu K, Okada A, Miyazawa T, Ohya M, Higashijima T (1992) Membrane-bound conformation of mastoparan-X, a G-protein-activating peptide. *Biochemistry* 31:5654–5660.
25. Shai Y (1999) Mechanism of the binding, insertion and destabilization of phospholipid bilayer membranes by α -helical antimicrobial and cell non-selective membrane-lytic peptides. *Biochim Biophys Acta* 1462:55–70.
26. Henriques ST, Melo MN, Castanho MA (2006) Cell-penetrating peptides and antimicrobial peptides: How different are they? *Biochem J* 399:1–7.
27. Paredes-Gamero EJ, Martins MNC, Cappabianco FAM, Ide JS, Miranda A (2012) Characterization of dual effects induced by antimicrobial peptides: Regulated cell death or membrane disruption. *Biochim Biophys Acta* 1820:1062–1072.
28. Talukder P, Chen S, Arce PM, Hecht SM (2014) Efficient asymmetric synthesis of tryptophan analogues having useful photophysical properties. *Org Lett* 16:556–559.
29. Francis D, Winn M, Latham J, Greaney MF, Micklefield J (2017) An engineered tryptophan synthase opens new enzymatic pathways to β -methyltryptophan and derivatives. *ChemBioChem* 18:382–386.
30. Lippitz M, Erker W, Decker H, van Holde KE, Basché T (2002) Two-photon excitation microscopy of tryptophan-containing proteins. *Proc Natl Acad Sci USA* 99:2772–2777.
31. Rehms AA, Callis PR (1993) Two-photon fluorescence excitation spectra of aromatic amino acids. *Chem Phys Lett* 208:276–282.
32. Palero J, Boer V, Vijverberg J, Gerritsen H, Sterenberg HJCM (2005) Short-wavelength two-photon excitation fluorescence microscopy of tryptophan with a photonic crystal fiber based light source. *Opt Express* 13:5363–5368.
33. Cohen DT, Buchwald SL (2015) Mild palladium-catalyzed cyanation of (hetero)aryl halides and triflates in aqueous media. *Org Lett* 17:202–205.
34. Schneider CA, Rasband WS, Eliceiri KW (2012) NIH Image to ImageJ: 25 years of image analysis. *Nat Methods* 9:671–675.

ACKNOWLEDGMENTS. We thank Drs. Samantha Wilner and Tobias Baumgart (University of Pennsylvania) for generously providing the HEK293T/17 cells and assisting with the wide-field imaging measurements. We acknowledge financial support from the National Institutes of Health (NIH) (P41-GM104605 and GM54616). M.R.H. is supported by a National Science Foundation Graduate Research Fellowship (DGE-1321851). I.A.A. is supported by a NIH T32 Interdisciplinary Cardiovascular Training Grant (T32-HL007954).